

A New Electrochemical Sensing Platform Based on Binary Composite of Graphene Oxide-Chitosan for Sensitive Rutin Determination

Majid Arvand¹ · Atefeh Shabani² · Masoomeh Sayyar Ardaki¹

Received: 22 October 2016 / Accepted: 2 January 2017 / Published online: 16 January 2017
© Springer Science+Business Media New York 2017

Abstract A new, simple, and low-cost voltammetric sensor was designed by covering a layer of graphene oxide/chitosan (GO–Cs) nanocomposite on a glassy carbon electrode (GCE). The synthesized GO nanosheets and GO–Cs nanocomposite were characterized by different techniques such as Fourier transform infrared spectroscopy (FT–IR), scanning electron microscopy (SEM), and transmission electron microscopy (TEM). The electrochemical behavior of rutin at the modified electrode was investigated, and the results demonstrated that the GO–Cs nanocomposite film could remarkably increase the redox peak current of rutin. The effects of supporting electrolyte, pH, accumulation parameters, and interference on the response of rutin were studied. Using differential pulse voltammetry (DPV) under optimized conditions, the analytical curve was linear in rutin concentration range from 0.9 to 90 $\mu\text{mol/L}$ with a detection limit of 0.56 $\mu\text{mol/L}$. The GO–Cs/GCE exhibited good selectivity and sensitivity for the determination of rutin content in real samples with satisfactory results.

Keywords Rutin · Graphene oxide · Chitosan · Nanocomposite · Film-modified electrode · Voltammetry

Introduction

Flavonoids are an important group of secondary metabolites and bioactive compounds in plants and well-known natural antioxidants in human diets (Kim et al. 2003). They are a kind of natural polyphenolic substances capable of scavenging free superoxide radicals. Hence, these compounds can effectively inhibit lipid peroxidation and prevent carbohydrates, proteins, DNA, and cells from oxidative damage (Wu et al. 2008). Flavonoids can be divided into various classes on the basis of their molecular structure. The most common classes are the flavones, flavonols, flavanones, catechins, isoflavones, and anthocyanidins. Rutin (3,4,5,7-tetrahydroxyflavone-3-d-rutinoside), also called rutoside, quercetin-3-O-rutinoside, and sophorin, is one of the most bioactive flavonoids. It is a citrus flavonoid glycoside between the flavonol quercetin and the disaccharide rutinose that for the first time was isolated from orange and designated as vitamin P (Nijveldt et al. 2001). Rutin is found in many fruits including orange, lemon, apple, berries, and grapes (Häkkinen et al. 1999; Anttonen et al. 2006). In vitro studies showed that rutin has several pharmacological functions such as antioxidant (Boyle et al. 2000), antithrombotic (Sheu et al. 2004), cytoprotective (Potapovich and Kostyuk 2003), vasoprotective (Tang et al. 2011), and cardioprotective activities (Ziaee et al. 2009). Thus, it is very important to develop simple, sensitive, and accurate analytical methods for detection and quantitation of rutin in plant sources and pharmaceutical samples. Many analytical methods have been developed for this purpose, including high-performance liquid chromatography (Brolis et al. 1998; Ishii et al. 2001), capillary electrophoresis (Chen et al. 2000; Chen et al. 2001), chemiluminescence (Song and Wang 2001), sequential injection analysis (Legnerova et al. 2003), spectrophotometric (Leng et al. 2013), and electrochemical methods (Yin et al. 2011; Liu et al. 2013; Miao et al. 2014).

✉ Majid Arvand
arvand@guilan.ac.ir

¹ Electroanalytical Chemistry Laboratory, Faculty of Chemistry, University of Guilan, Namjoo Street, P.O. Box: 1914-41335, Rasht, Iran

² Department of Chemistry, Payame Noor University, Tehran, Iran

Compared with other methods, electrochemical methods are characterized by portability, simplicity, minimal cost, and short analysis time (Zhu et al. 2010; de Oliveira et al. 2006). Furthermore, due to the fact that rutin is an electroactive species, considerable efforts have been devoted to develop voltammetric methods for its determination in the recent years. Various working electrodes, including glassy carbon electrode (GCE) (Hendrickson et al. 1994a, b; Hendrickson et al. 1994a, b), poly(vinylpyrrolidone)-modified carbon paste electrode (Franzoi et al. 2008), ionic liquid-modified carbon paste electrode (Sun et al. 2008), DNA-modified carbon paste electrode (Wang et al. 2010), and single-walled carbon nanotube-modified gold electrode (Zhang et al. 2007), had been used for the electrochemical determination of rutin. Because of production of passivating polymeric film at bare solid electrodes and decrease of sensitivity and selectivity, electrochemical determination of rutin on unmodified electrodes such as GCE and carbon paste electrode is limited (Pinar et al. 2013). Therefore, a large number of papers in the literature involve the use of modified electrodes (Freitas et al. 2009; Franzoi et al. 2009). Recently, chemically modified electrodes have attracted a lot of attention due to the possibility of modifying the electrode surface including polymer coating, composite generation, and so forth. And the sensitivity, selectivity, and operational stability of electrochemical analysis can be enhanced using these electrodes (Fatibello-Filho and Vieira 2000; Ferreira Batista et al. 2010). To our knowledge, no study related to the determination of rutin using a graphene oxide-chitosan film-modified electrode has appeared in the literature.

Graphene oxide (GO), an important derivative of graphene, is a two-dimensional sheet-shaped carbon nanostructure that has large amount of oxygen functional groups (hydroxyl, carboxyl, and epoxy groups) on its basal plane and edges. It is considered as a special and new material possessing a high area to volume ratio, violent charge transport, and good electrocatalytic properties (Jang et al. 2013; Mani et al. 2013). In addition, due to the presence of the oxygen functionalities, GO shows excellent hydrophilicity and is relatively easily dispersed in water and other organic solvents as well as in different matrixes (Yang et al. 2014). This remains as a very important property when mixing it with polymer matrixes and trying to further improve its chemical, physical, and electrical properties. These novel properties can be made GO greatly promising for the various applications such as sensors (Sharma et al. 2013; Balapanuru et al. 2010), high functional batteries (Rao et al. 2011), solar energy system (Zhu et al. 2011), and highly sophisticated microelectrical devices (Jin et al. 2009).

Chitosan (Cs) is a polysaccharide comprising copolymers of glucosamine and N-acetylglucosamine and obtained from marine chitin. It contains large groups of $-\text{NH}_2$ and $-\text{OH}$ and is soluble in aqueous acidic media at $\text{pH} < 6.5$. The Cs can

adhere to negatively charged surfaces or adsorb negatively charged materials when dissolved and carried with the positive charge of $-\text{NH}_3^+$ groups (Kang et al. 2009; Xu et al. 2001; Jiang et al. 2005). It is commonly used to disperse nanomaterials and as a modifying reagent to prepare modified electrode due to its excellent capability for film formation, non-toxicity, easy-handling, cheapness, and high mechanical strength (Kang et al. 2009).

In the present work, a simple, low-cost, and practical analytical approach is illustrated on determination of rutin in pistachio and five fruit samples. A modified GCE with hybrid nanocomposite of GO-Cs was used for this task. The excellent properties of GO-Cs nanocomposite film effectively facilitate the adsorption of rutin on the surface of the modified electrode and improve sensitivity in the determination of this flavonoid in real samples.

Experiment

Reagents and Solutions

All the chemicals were of analytical reagent grade and used as received without further purification. Chitosan was obtained from Sigma-Aldrich Chemical Co. Rutin, graphite powder (99.999% purity, -200 mesh), ethanol (99.9% v/v), potassium chlorate, fuming nitric acid (90% w/w), and glacial acetic acid were purchased from Merck (Darmstadt, Germany). Aqueous solutions were prepared with citrate buffer solution (CBS) 0.1 mol/L (pH 4.5) by mixing solutions of 0.1 mol/L sodium citrate and 0.1 mol/L citric acid. The stock solution of rutin (1 mmol/L) in ethanol/NaOH (50% v/v) was prepared daily and just before use. Double-distilled water was used for the preparation of all the solutions.

Apparatus

The electrochemical measurements were performed with an Autolab PGSTAT 30 electrochemical analyzer (Eco Chemie BV, Utrecht, the Netherlands). All electrochemical studies were performed at 25 ± 1 °C. Three-electrode cell systems were used to monitor the cyclic and differential pulse voltammograms. A saturated Ag/AgCl electrode, a platinum wire, and a modified GCE were used as the reference, auxiliary, and working electrodes, respectively. All the pH solutions were measured via the Metrohm pH meter (model 827, Swiss made). Scanning electron microscope (SEM) images were obtained with LEO 1430VP. A model CM10 transmission electron microscope (TEM; Philips) was used to characterize the morphology and size of the GO nanosheets. Fourier transform infrared (FT-IR) spectra of GO, Cs, and GO-Cs nanocomposites were obtained using a Shimadzu 8900 spectrometer. All UV-Vis absorption spectra of the samples were

recorded using a Biochrom WPA Biowave II UV-Vis spectrophotometer in the range of 200–900 nm.

Synthesis of GO

GO was synthesized based on our previous report (Arvand and Gholizadeh 2013). In brief, 1.0 g of pure graphite and 8.0 g of potassium chlorate were mixed in 20 mL of fuming nitric acid at room temperature without subsequent aging and stirred for 24 h. The following processes such as washing, filtration, and cleaning were carried out as in Brodie method. The obtained graphite oxide was dispersed in aqueous NaOH solution (pH 10) with a certain concentration and subsequently sonicated to obtain GO. After ultrasonication, samples were immediately precipitated by a centrifuge at 14,000 rpm for 10 min and the GO nanosheets were extracted carefully.

Preparation of Modified Electrodes

Prior to the surface modification, the GCE was polished to mirror-like surface with alumina powder and then washed with 1:1 double-distilled water and ethanol in an ultrasonic bath and dried in room temperature. At first, the Cs solution (2.0% w/v) was prepared by dissolving 0.2 g of Cs in 10 mL acetic acid (0.02 mol/L) and was stored in a refrigerator when not in use. Of the GO suspension (1% w/v), 250 μ L was mixed thoroughly with 100 μ L Cs solution. Next, 10 μ L of GO–Cs dispersion was dropped on the surface of GCE and dried in air. Finally, to get more uniform films, 7 μ L of the above mixture was again dropped onto the GCE surface, and then, the solvent was allowed to evaporate at room temperature. To compare with GO–Cs/GCE, GO/GCE was also fabricated according to the same casting method.

Sample Preparation

Pistachio

Raw pistachio nuts, harvested in Damghan, Iran, were obtained from local market. They were dried at 37 °C overnight and then pulverized in a mill within 15 min to a final fineness of 95% below 5 mm. Next, an accurate weight amount of the powder (2.0 g) was added to 70% (v/v) ethanol (40 mL), and the suspension was placed in an 80 °C water bath and the solution was stirred for 3 h. After cooling, the mixture was centrifuged for 5 min and filtered with Whatman filter paper.

Fruit Samples

Fruit samples including golden apple, red grape, sour cherry, black mulberry, and strawberry were purchased from local grocery stores in Rasht city and were utilized for production of varietal juices. Each sample was crushed in mixer, and the

obtained mixtures were consisted of juice, pulp, and skin. For rutin extraction, 20 mL of each sample was added to 40 mL of 70% (v/v) ethanol and heated at 80 °C in water bath for 3 h with regular swirling. Samples were removed from the water bath and cooled to room temperature. The supernatant layer of each sample was filtered through a paper filter into a vial and stored at 4 °C in a refrigerator until analysis.

Electroanalytical and UV-Vis Spectrophotometric Measurements

The analytical procedure mainly contains the following two steps: accumulation of rutin at the proposed electrode surface and determining step. The obtained results indicated that rutin molecules could be completely removed from the electrode surface in alkaline medium. This might be explained that alkaline environment could increase the solubility of rutin. Therefore, after each measurement, the GO–Cs/GCE undergoes five cyclic sweeps in 0.1 M NaOH to remove any adsorbates and give a reproducible electrode surface. The pulse amplitude of 0.025 V, pulse interval time of 0.5 s, and scan rate of 0.01 V/s were selected as optimum instrumental parameters for differential pulse voltammetry (DPV) measurements.

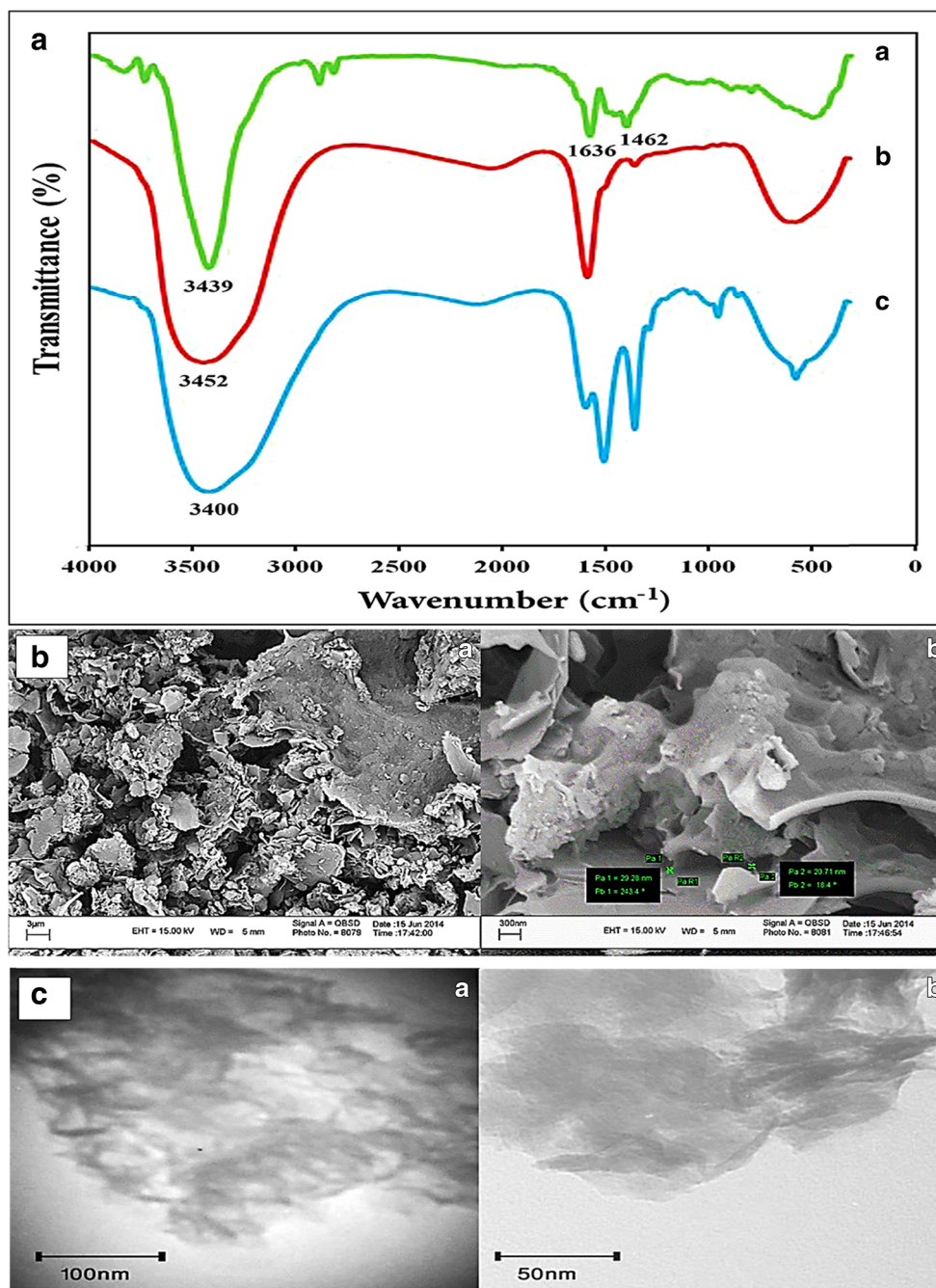
UV-Vis spectra were measured at wavelengths ranging from 200 and 900 nm immediately after preparation of the solutions. Similar to other phenolic compounds, rutin shows two absorption bands between 200 and 360 nm. The absorbance measurements were performed at 355 nm against the 0.1 M CBS as a blank solution in this work. Prior to the analysis of the real samples, the calibration curve as absorbance vs. concentration was constructed to study the Beer-Lambert's law and regression equation for rutin.

Results and Discussion

FT-IR Characterization

Figure 1a shows the FT-IR spectra of GO nanosheets (a), Cs (b), and GO–Cs nanocomposite (c). The spectrum of GO has two characteristic peaks at 3439 cm^{-1} from hydroxyl group and at 1636 cm^{-1} from carbonyl group, which indicates the presence of oxygen-containing functional groups and confirms the successful oxidation of graphite. Peak at 1462 cm^{-1} corresponds to skeletal vibrations from non-oxide graphitic domains. The spectrum of GO–Cs nanocomposite shows the characteristic bands of the parent molecules. Compared with the spectrum of Cs, the band corresponding to the O–H and N–H stretching modes (3452 cm^{-1}) is broader and shifts to a lower wave number (3400 cm^{-1}). These could be ascribed to the synergistic effect of hydrogen bonding between GO and Cs, and electrostatic interaction between the

Fig. 1 **a** FT-IR spectra of GO (a), Cs (b), and GO–Cs (c) nanocomposite; **b** SEM images of GO nanosheets in scale of 3000 (a) and 300 nm (b), orderly; and **c** TEM images of GO nanocomposite in scales of 100 (a) and 50 nm (b)



NH_3^+ groups of Cs and the negative charge on the surface of GO, which prevented GO nanosheets from aggregation in Cs solution and improved its chemical, physical, and electrical properties (Yang et al. 2010; Feng et al. 2013).

Morphology of GO Nanosheets

The structural morphology of the GO nanosheets was examined by SEM and TEM. Figure 1b shows the typical SEM images of GO with different magnifications. It is apparent that GO nanosheets are flake-like with exposed sharp edges. The

edges are stabilized through a number of chemical functionalities including hydroxyl and carbonyl groups that can undergo redox reactions in solution (Notley et al. 2013). These observations indicate that GO nanosheets were successfully synthesized and can obviously improve the electrocatalytic performance of the proposed electrode. Figure 1b also implies that GO sheets form a porous network which increase the effective surface area of the modified electrode and facilitate the adsorption of analyte on the nanocomposite film. Figure 1c exhibits two TEM images of GO nanosheets with different magnifications. They show a wrinkled texture that

was associated with the presence of flexible and ultrathin nanosheets. These wrinkles may be important for maintaining high surface area and for preventing aggregation of GO due to van der Waals forces (Sun et al. 2013). And, from the SEM and TEM images, it was concluded that the thickness of GO nanosheets was lower than 60 nm.

Electrochemical Properties of Modified Electrodes

The electrochemical performance of GO/GCE and GO–Cs/GCE were investigated using a solution of 5 mmol/L $[\text{Fe}(\text{CN})_6]^{3-/4-}$ redox probe at scan rate of 0.1 V/s. As can be seen in Fig. 2a, a pair of redox peaks with ΔE_p of 0.290, 0.131, and 0.543 V were observed at GO–Cs (dashed dotted line), GO (dotted line), and bare (solid line) glassy carbon electrodes, respectively. The reduction in ΔE_p value at GO–Cs/GCE clearly indicated the more-reversible charge-transfer process of GO–Cs/GCE than GCE. The anodic peak current (I_{pa}) of GO–Cs/GCE was found to be 8 and 20.5 times higher than GO modified and bare GCE, orderly, suggesting that GO–Cs/GCE exhibits faster electron-transfer kinetics and larger electroactive surface area compared to GO/GCE and GCE. Therefore, it can be concluded that GO and Cs have synergistic effect. The effective surface area of the electrodes was obtained by CV using the $[\text{Fe}(\text{CN})_6]^{3-/4-}$ redox system. For a reversible process, the following Randles-Sevcik formula can be used (Bard and Faulkner 2004):

$$I_p = (2.69 \times 10^5) A n^{3/2} D^{1/2} C_0 \nu^{1/2} \quad (1)$$

where I_p refers to the peak current (A), A is the surface area of electrode (cm^2), $n = 1$ for $\text{K}_3\text{Fe}(\text{CN})_6$, D is the diffusion coefficient ($7.6 \times 10^{-6} \text{ cm}^2/\text{s}$), ν is the scan rate (V/s), and C_0 is the concentration of $\text{K}_3\text{Fe}(\text{CN})_6$ in mol/L. The slope of I_p vs. $\nu^{1/2}$ plot was then used to calculate the surface area of bare and modified electrodes, which were found as 0.01, 0.05, and 0.16 cm^2 for GCE, GO/GCE, and GO–Cs/GCE, respectively. These results indicate a significant enhancement in surface area after modification with GO–Cs nanocomposite. The high specific surface area of GO and the unique properties of Cs such as more effective distribution of GO nanosheets and different GO flake arrangement in Cs solution were helpful for promoting the electrochemical signals (Celiešiūtė et al. 2013; Banks et al. 2006).

Electrochemical Behavior of Rutin at Modified Electrode

Figure 2b shows the cyclic voltammograms of 100 $\mu\text{mol/L}$ rutin on different electrodes in CBS (pH 4.5). Both on GO/GCE (curve a) and GO–Cs/GCE (curve b and inset), a pair of well-defined redox peaks appeared, indicating that the electrochemical reaction of rutin take place on these electrodes. As shown in Fig. 2b, the cyclic

voltammograms of rutin show a peak-to-peak separation (ΔE_p) of 0.122 and 0.051 V at the surface of GO/GCE and GO–Cs/GCE, respectively. This observation suggests faster electron transfer kinetics for rutin at GO–Cs nanocomposite-modified electrode. The voltammograms in Fig. 2b clearly depict that compared with GO–Cs/GCE, GO/GCE did not show a considerable change in the redox peak current, while its background current was higher than that of the GO–Cs/GCE. These results indicated that the improved electrochemical behavior of rutin at GO–Cs/GCE mainly attributed to the synergistic effect of GO and Cs. The synergistic effect occurred due to the relatively high area to volume ratio and violent charge transport properties of GO and some intermolecular interactions between Cs and rutin such as hydrogen bonding (Feng et al. 2013). As mentioned in the FT–IR Characterization, Cs can interact with GO by formation of hydrogen bond and electrostatic interaction, which resulted in the formation of a stable GO film-modified electrode.

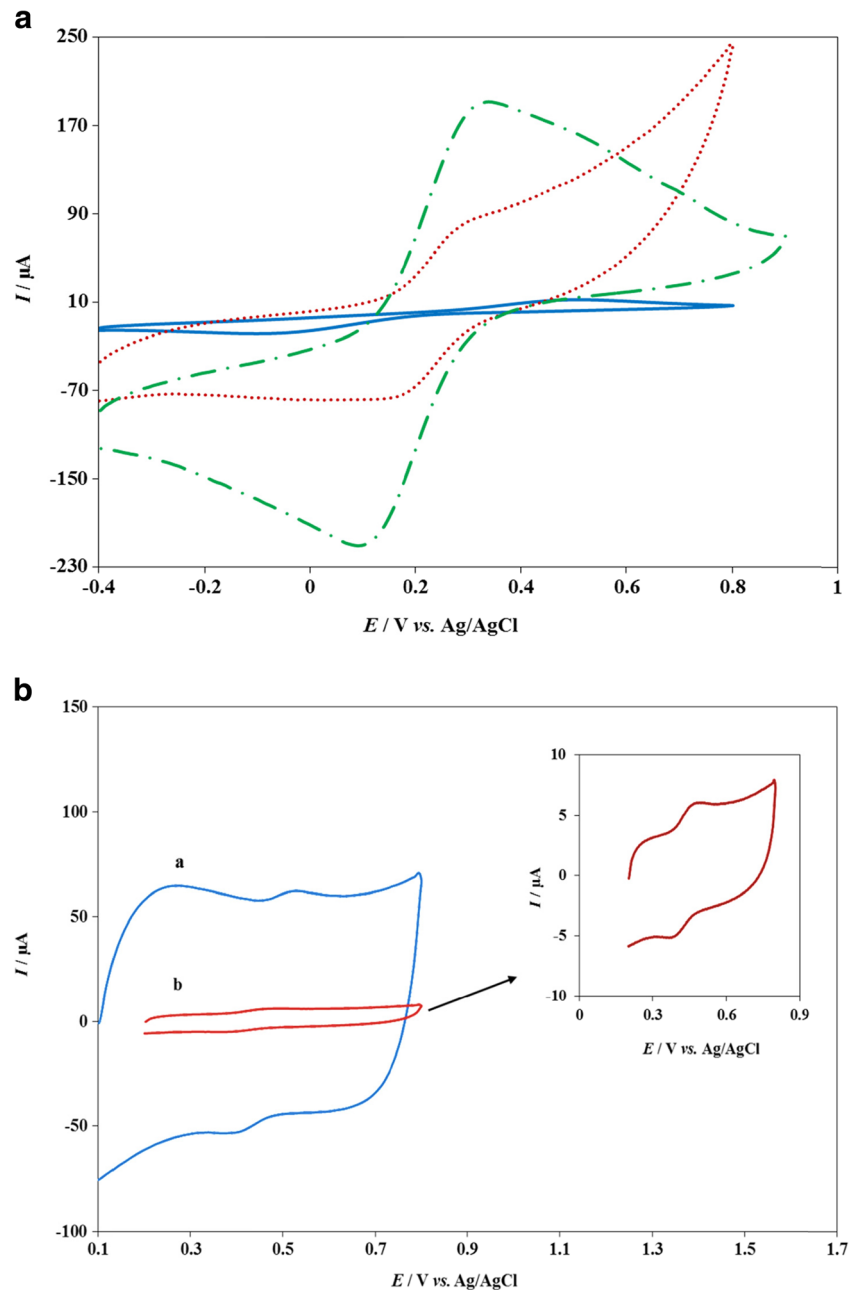
Effect of Scan Rate

The effect of scan rate on the electrochemical response of 100 $\mu\text{mol/L}$ rutin at the GO–Cs/GCE was investigated by cyclic voltammetry (Fig. 3a). It can be seen that the redox peak current increases linearly with the scan rate in the range of 0.01–0.2 V/s. The linear regression equations $I_{pa} (\mu\text{A}) = 23.509\nu (\text{V/s}) - 0.2055$ ($R^2 = 0.9982$) and $I_{pc} (\mu\text{A}) = 17.136\nu (\text{V/s}) - 0.1549$ ($R^2 = 0.9980$), respectively, implied that the electrocatalytic reaction was adsorption controlled (Fig. 3b). Furthermore, a plot of log peak current vs. log scan rate for the anodic peak is also linear (Fig. 3b, inset a). The linear equation can be defined as $\log I_{pa} (\mu\text{A}) = 0.9246 \log \nu (\text{V/s}) + 1.3344$. The value of its slope (0.9246) is close to the theoretical value of 1, which clearly indicates an adsorption-controlled electrode process. Similarly, the redox potential had a linear relationship with the logarithm of scan rate, and the regression equations were $E_{pa} (\text{V}) = 0.0526 \log \nu (\text{V/s}) + 0.4987$ and $E_{pc} (\text{V}) = 0.0254 \log \nu (\text{V/s}) + 0.4134$ with $R^2 = 0.9542$ and 0.9858, respectively. According to the Laviron's equation (Laviron 1974), for an adsorption-controlled and quasi-reversible interfacial reaction, the relationship between E_{pa} and ν is defined by the following equation:

$$E_{pa} = K + \left[\frac{2.303RT}{(1-\alpha)nF} \right] \log \nu \quad (2)$$

where α is the charge transfer coefficient, ν is the scan rate, and K is a constant value. From the slope of E_{pa} vs. $\log \nu$ plot, the value of $(1-\alpha)n$ was found to be 1.13. In order to obtain charge transfer coefficient, the Tafel plot was drawn using the rising part of the current–voltage curve of rutin monitored at

Fig. 2 **a** Cyclic voltammograms of the GO–Cs/GCE (dashed dotted line), GO/GCE (dotted line), and bare GCE (solid line) in 5 mmol/L $K_3[Fe(CN)_6]$ containing 0.1 mol/L KCl. **b** Cyclic voltammograms of the GO/GCE (a) and GO–Cs/GCE (b) in a 0.1 mol/L CBS (pH 4.5) containing 100 $\mu\text{mol/L}$ rutin (scan rate 0.1 V/s)



scan rate of 0.01 V/s (Fig. 3b, inset b). This part of voltammogram, known as Tafel region, is affected by electron transfer kinetics between rutin and GO–Cs/GCE. The slope of this plot was 0.1176 V/decade that indicates a charge transfer coefficient of $\alpha = 0.497$. Therefore, the number of electrons involved in the electrode reaction was calculated to be 2.0.

Optimization of Measurement Parameters

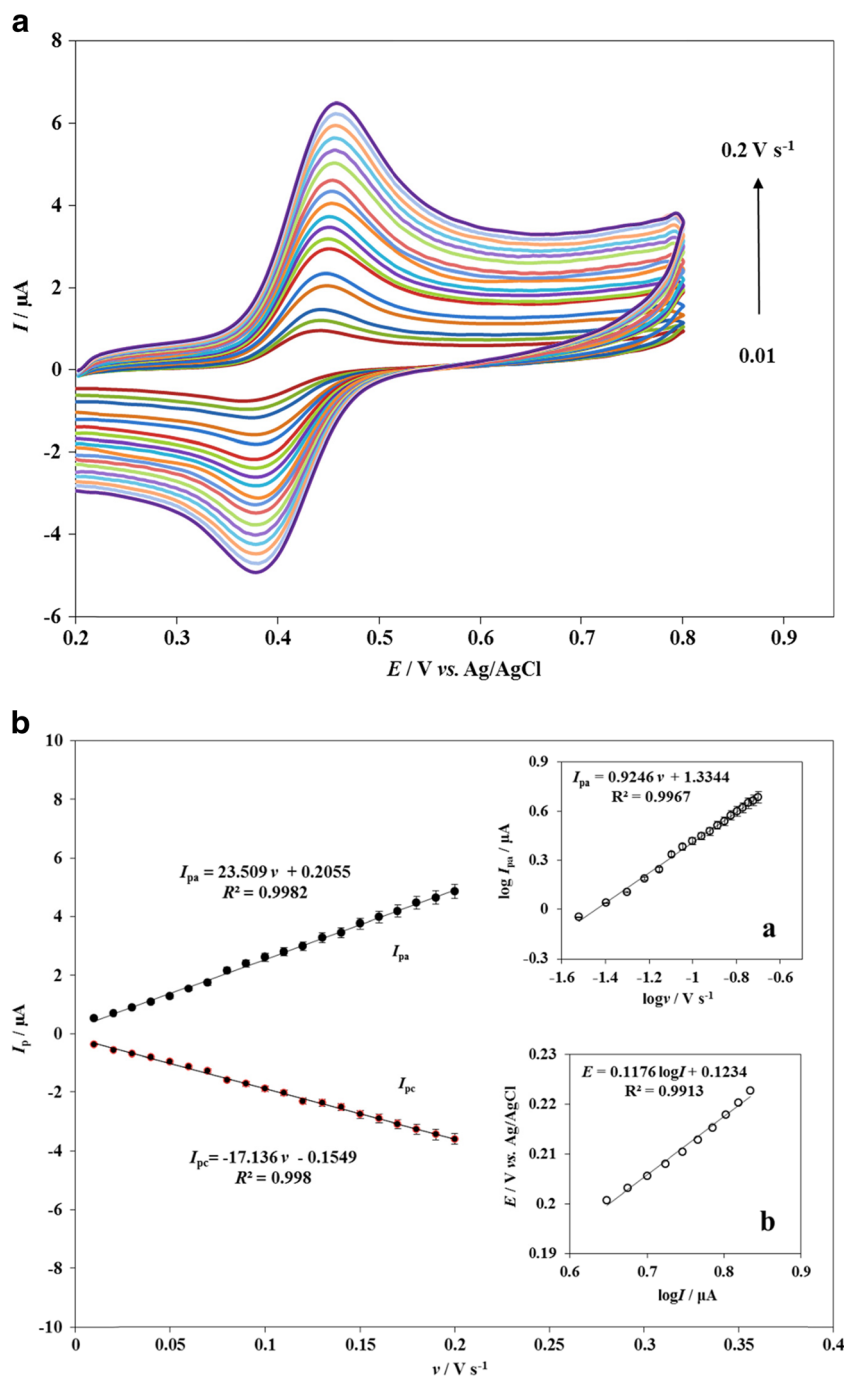
Influence of Supporting Electrolyte and pH

According to previous studies, type of supporting electrolyte and its pH play a key role in the voltammetric response of

rutin. To optimize the response of the proposed electrode, various supporting electrolytes such as phosphate, acetate, and citrate buffer solution (each 0.1 mol/L) were investigated using cyclic voltammetry. The results showed that the GO–Cs nanocomposite film has very low mechanical stability in acetate buffer solution and the best waveform and maximum redox peak currents were obtained using 0.1 M CBS solution. The reason may be that the interaction between rutin and the GO–Cs nanocomposite film was more favored in CBS. Therefore, 0.1 M CBS was selected as the electrolyte for further experiments.

The influence of pH on the voltammetric response of 100 $\mu\text{mol/L}$ rutin was investigated in the pH range of 3.5 to

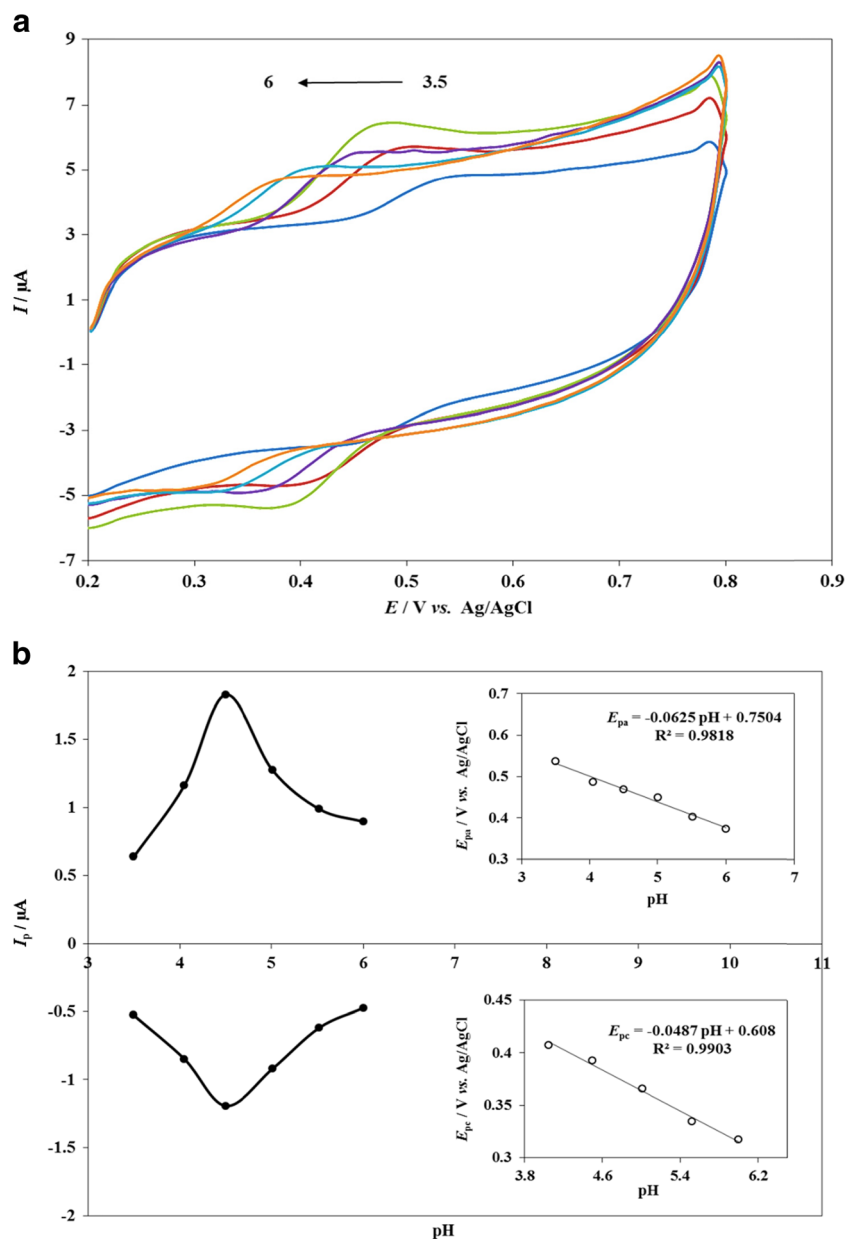
Fig. 3 **a** Cyclic voltammograms of 100 $\mu\text{mol/L}$ rutin in 0.1 mol/L CBS (pH 4.5) on the surface of GO–Cs/GCE at different scan rates. **b** Linear relationship of anodic and cathodic peak currents (I_p) vs. scan rate. *Inset a* is the relationship between the logarithmic peak current and the logarithmic scan rate for the anodic peak. *Inset b* is the Tafel plot derived from the current potential curve recorded at scan rate of 0.01 V/s



6.0 (Fig. 4a). Variations of redox peak current with respect to pH of the electrolyte are shown in Fig. 4b. As can be seen, the peak current was increased gradually with increasing pH and reached maximum value at pH 4.5. Further increasing the pH of the buffer solution caused the redox peak current to decrease. These phenomena might be due to the interaction between the electrode surface and the analyte charges. At low pH value, rutin has cationic form and the negative functional groups of GO–Cs nanocomposite started attracting rutin cations to the electrode surface. Above pH 4.5, the degree of protonation of rutin was decreased. The decrease in rutin cations resulted in

less interaction between it and nanocomposite film. On the other hand, when pH varied from 3.5 to 6.0, the peak potential of rutin redox shifted linearly to the negative direction, implying that protons took part in the electrode reaction (inset of Fig. 4b). From the slopes of the E_p –pH plots (0.0625 and 0.0487), it could be concluded that equal number of protons and electrons is involved in the electrode reaction at the modified electrode. As mentioned in the section **Effect of Scan Rate**, the number of electrons transferred in electrode reaction was 2. Combining the former result that the identical number of protons and electrons were transferred in the electrochemical

Fig. 4 **a** Cyclic voltammograms for GO–Cs/GCE in 0.1 mol/L CBS containing 100 $\mu\text{mol/L}$ rutin at different pH values of 3.5, 4.0, 4.5, 5.0, 5.5, and 6 (scan rate 0.1 V/s). **b** Variations of redox peak current (I_p) with respect to pH of the electrolyte. *Inset* is the linear relationship of anodic and cathodic peak potentials (E_p) vs. pH



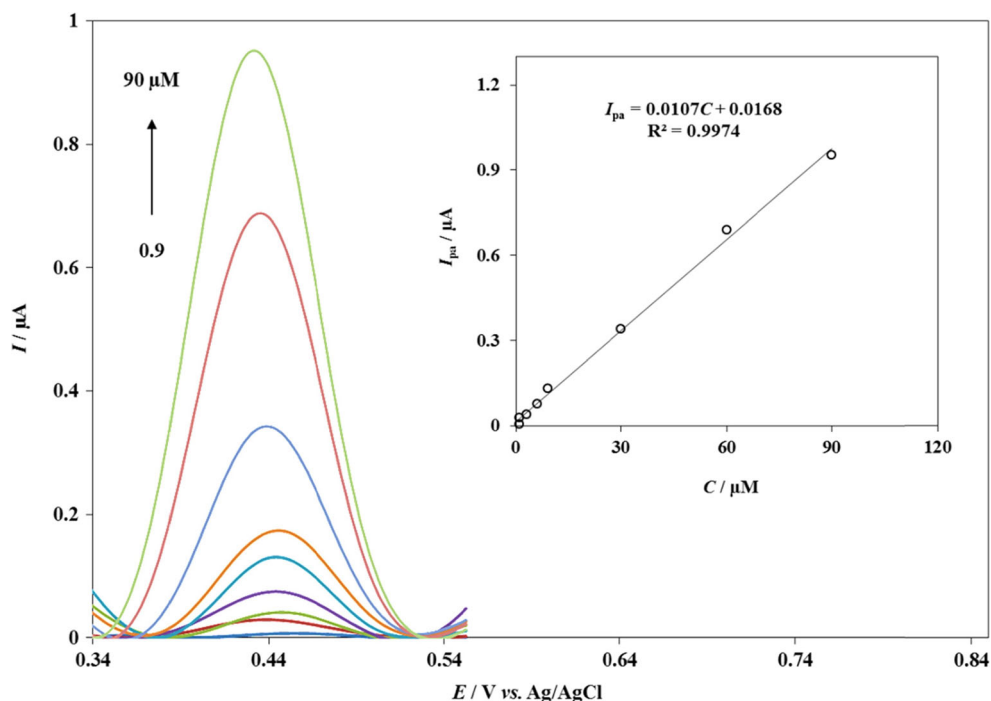
reaction, the electrooxidation reaction of rutin belonged to a two-electron and two-proton process, which is consistent with the previous reports for it (Zhu et al. 2010; da Silva et al. 2012).

Effect of Accumulation Time and Accumulation Potential

Because the electrode reaction of rutin is an adsorption driven process on the GO–Cs/GCE, two parameters of accumulation step can improve the preconcentration of rutin on the electrode surface and obviously enhance sensitivity. Therefore, the influence of accumulation time on the oxidation peak current of

25 $\mu\text{mol/L}$ rutin was studied at CBS (pH 4.5) using DPV under open circuit conditions. The anodic peak current was reached the maximum value after immersing GO–Cs/GCE into solution after 25 s. Thus, the 25 s was chosen as the optimal accumulation time for further study. At this accumulation time, the effect of accumulation potential on the peak current was investigated over the range of -0.2 to 0.15 V. The peak current was increased gradually until accumulation potential reached a value of -0.1 V and then decreased. Therefore, the accumulation step in the experiments was performed at -0.1 V for 25 s.

Fig. 5 DPVs obtained at the GO–Cs/GCE for rutin (CBS, pH 4.5) at different concentrations from 0.9 to 90 $\mu\text{mol/L}$. *Inset* is the calibration curve of rutin



Analytical Performance

Under optimized conditions, the relationship between the anodic peak current and the concentration of rutin was studied using DPV (Fig. 5). The proposed sensor shows a linear response toward rutin in the concentration range from 0.9 to 90 $\mu\text{mol/L}$ (inset of Fig. 5). This linear relationship can be expressed according to the following equation:

$$I_{\text{pa}} = 0.0107C + 0.0168 \quad (R^2 = 0.9974) \quad (3)$$

where I_{pa} is the anodic peak current (μA) and C is the rutin concentration ($\mu\text{mol/L}$). The limit of detection (LOD) and

quantification (LOQ) were calculated using the following equations:

$$\text{LOD} = \frac{3S_b}{m}; \quad \text{LOQ} = \frac{10S_b}{m} \quad (4)$$

where S_b is the standard deviation of the blank (five runs) and m is the slope of the calibration curve. The proposed method showed LOD and LOQ of 0.56 and 1.88 $\mu\text{mol/L}$, orderly. The repeatability of this method was investigated by relative standard deviation (RSD) of intra-day and inter-day repeatability. The intra-day repeatability was estimated by assaying one GO–Cs/GCE for five replicate measurements of 25 $\mu\text{mol/L}$ rutin under uniform conditions, and the RSD value was calculated to be 1.81%. The

Table 1 Comparison of the proposed electrode with other electrodes for the determination of rutin

Electrode	Method	Linear range ($\mu\text{mol/L}$)	LOD ($\mu\text{mol/L}$)	References
SWCNTs/CILE	DPV	0.10–800.00	0.07	Zhu et al. (2010)
Enzyme/Cs/CPE	SWV	0.30–7.20	0.02	de Oliveira et al. (2006)
PVP/CPE	LSV	0.39–13.00	0.15	Franzoi et al. (2008)
CCEM–Cu(II)–resin	LSV	0.99–8.07	0.03	Freitas et al. (2009)
DMI–Tf ₂ N–laccase/CPE	SWV	5.84–53.60	0.69	Franzoi et al. (2009)
HMDE	DPV	0.20–1.40	–	da Silva et al. (2012)
GO–Cs/GCE	DPV	0.90–90.00	0.56	This work

CILE carbon ionic liquid electrode, CCEM carbon–composite electrode modified

Table 2 Tolerance of interferences on the determination of rutin

Foreign species	Tolerance level ratio
Mg ²⁺ , Na ⁺ , Ca ²⁺ , and K ⁺	500
Glucose and sucrose	200
Ascorbic acid	10
Quercetin	4

inter-day repeatability was also assessed using 25 $\mu\text{mol/L}$ rutin, but several measurements were made over 3 days, yielding RSD value of 3.19%. The obtained results revealed that this method has good repeatability. When three GO–Cs electrodes fabricated by the same method were used for the measurement of a 25 $\mu\text{mol/L}$ rutin solution, the RSD of the peak current was 3.5%, which indicates that the electrode has good reproducibility. A comparison between the analytical performance of the GO–Cs/GCE and some previous literature electrodes for rutin determination was given in Table 1. As can be seen, the proposed electrode showed a wide linear range and comparable LOD than those obtained at several electrodes. Although in reported methods lower LODs have been reported, they used carbon nanotubes, ionic liquid, and enzyme as enhancing agents. These are more complex procedures compared to the method proposed in this work, which has a good LOD without the use of a

compound of these classes. In addition, the fabrication of proposed electrode was simple and fast, and it showed high stability and remarkable voltammetric reproducibility. Furthermore, it is important to note that the analytical parameters obtained in this work are sufficient to quantify rutin in real samples, as will be presented in the “Application” section.

Interference Test

It is well known that some coexistent interference substances in real samples may influence the performance of a sensor. Therefore, in order to evaluate the antiinterference ability of the proposed sensor, the influence of foreign species such as glucose, ascorbic acid, sucrose, quercetin, Mg²⁺, K⁺, Na⁺, and Ca²⁺ on the determination of rutin (24.5 $\mu\text{mol/L}$) was investigated by DPV. The tolerance limit was set as the maximum concentration of the foreign species, which caused an approximately $\pm 10\%$ relative error in the determination. The results are presented in Table 2. As shown in this table, it can be seen that fourfold excess of quercetin had no effect on the peak current of rutin. Figure 6 demonstrates the DPV curves of 24.5 $\mu\text{mol/L}$ rutin (a), the mixture of 90 $\mu\text{mol/L}$ quercetin and 24.5 $\mu\text{mol/L}$ rutin (b), and the mixture of 128 $\mu\text{mol/L}$ quercetin and 24.5 $\mu\text{mol/L}$ rutin (c) in CBS (pH 4.5) on the modified sensor. It can be seen that only one oxidation peak (at 0.44 V) was

Fig. 6 DPVs for rutin (24.5 $\mu\text{mol/L}$) and quercetin at GO–Cs/GCE. The quercetin concentrations in 0 (a), 90 (b), and 128 $\mu\text{mol/L}$ (c). Other conditions are the same as in Fig. 3

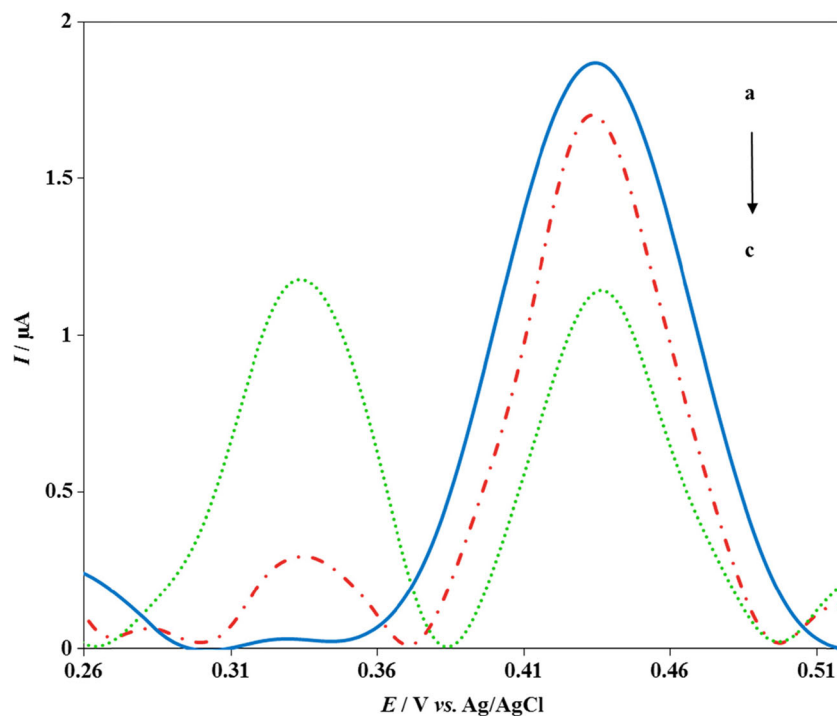
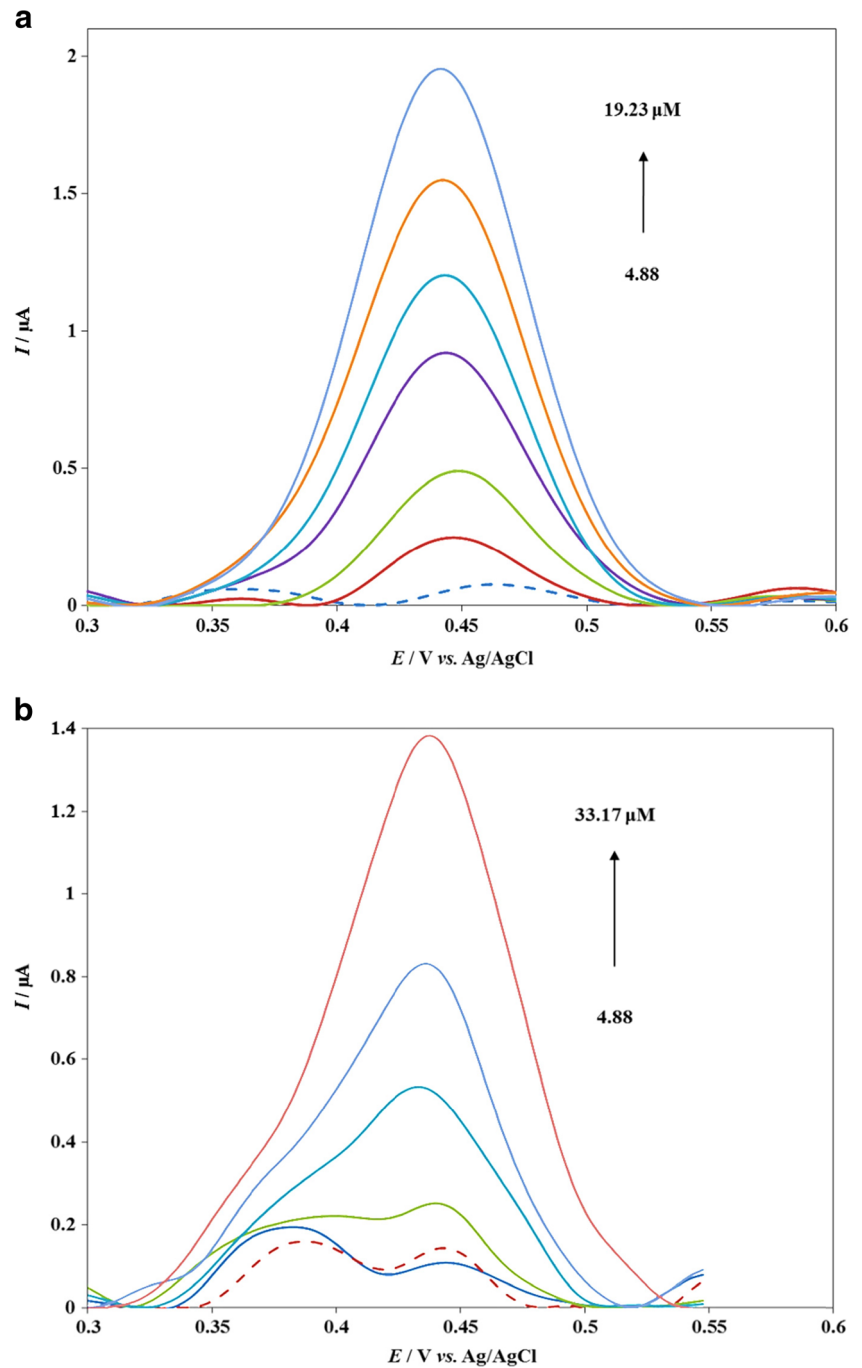


Fig. 7 DPVs obtained for **a** pistachio and **b** black mulberry samples in CBS (0.1 mol/L, pH 4.5) before (*dashed line*) and after spiking with different rutin concentrations



observed in the absence of quercetin, which was attributed to the oxidation of rutin. When quercetin was added, two anodic peaks were achieved with the peak potential of 0.33 and 0.44 V. The observed oxidation peak at 0.33 V is assigned to the oxidation of quercetin since this peak increases while adding quercetin standard solution. The peak-to-peak separation of quercetin and rutin was 0.11 V, which is enough for their simultaneous electrochemical determination. However, the separation of two

anodic peaks will improved by optimization of the effective experimental factors of mixed solution.

Application

In order to evaluate the validity of the proposed method, the fabricated electrode was used to determine rutin concentration in pistachio, golden apple, sour cherry, red grape, black

Table 3 Results of rutin determination in real samples by DPV compared with spectroscopic method

Sample	Rutin found Present method ^a (g/μL)	RSD (%)	Reference method (g/μL)	RSD (%)	<i>t</i> test ^b	<i>F</i> test ^c
Pistachio	467.1 ± 1.7	0.4	1.5 ± 462.7	0.3	3.4	1.3
Golden apple	623.6 ± 1.6	0.3	1.6 ± 618.5	0.3	3.9	1.0
Sour cherry	978.6 ± 2.3	0.2	978.0 ± 1.7	0.2	0.4	1.8
Red grape	2135.3 ± 2.0	0.1	2141.0 ± 1.8	0.1	3.7	1.2
Black mulberry	2206.4 ± 2.6	0.1	2213.7 ± 2.5	0.1	3.5	1.1
Strawberry	1880.4 ± 2.5	0.1	1884.1 ± 2.4	0.1	1.9	1.1

^a $x = \bar{x} \pm S_x$ for $n = 3$. S_x denotes standard deviation

^b Tabulated *t* value for 2° of freedom at *P* value of 0.05 is 4.30

^c Tabulated *F* value for 2, 2° of freedom at *P* value of 0.05 is 19.00

mulberry, and strawberry samples. A standard addition method was employed to evaluate the determination results. Figure 7 shows the DPVs obtained for pistachio and black mulberry samples in CBS (0.1 mol/L, pH 4.5), with different rutin concentrations. As can be seen from Fig. 7a, a well-defined peak at around 0.45 V was observed with the addition of appropriate amount of the aqueous ethanolic extract of pistachio, while two well-defined oxidation peaks appeared on the modified sensor for black mulberry solution (Fig. 7b). It is clearly shown that the observed oxidation peak at around 0.45 V is assigned to the oxidation of rutin since this peak increases while adding rutin standard solutions. The obtained results in above section suggested that the other oxidation peak in DPVs of black mulberry sample may be corresponding to the oxidation of quercetin. This finding confirms that the proposed sensor can be successfully applied in the simultaneous determination of rutin and quercetin in real samples. The results for detection of rutin in six samples are presented in Table 3. As can be seen in this table, the accuracy of the proposed method was compared to reference UV-Vis spectrophotometric method. By evaluation of these results, it can be concluded that the values obtained by the voltammetric method agree well with those acquired by the spectrophotometric method. The statistical calculations indicate good agreement between the mean values (*t* test) and precision (*F* test) for the two methods (for *P* = 0.05).

Conclusion

In this article, a new, simple, sensitive, and low-cost voltammetric sensor, GO–Cs/GCE, was proposed with high selectivity for rutin detection. GO has a large surface to volume ratio and high electron transmission rate, which improves significantly the sensitivity of modified electrode. The results indicate that Cs also plays an important role in forming a well-dispersed GO suspension and can significantly increase the adsorption of rutin on the surface of GO–Cs nanocomposite

film. Under the optimized conditions, the anodic peak current was linear to rutin concentration in a wide linear range (0.9–90 μmol/L), and the detection limit was about 0.56 μmol/L. Rutin content was successfully determined at this electrode in pistachio and five fruit samples using DPV, and the obtained results were in close agreement with those obtained using the spectrophotometric method at a 95% of confidence level.

Acknowledgements The authors are thankful to the post-graduate office of Guilan University for the support of this work.

Compliance with Ethical Standards

Funding This study was funded by Guilan University.

Conflict of interest M. Arvand declares that he/she has no conflict of interest. A. Shabani declares that he/she has no conflict of interest. M. Sayyar Ardaki declares that he/she has no conflict of interest.

Ethical Approval All procedures performed in studies were in accordance with the ethical standards of the institutional and/or national research committee and with the 1964 Helsinki declaration and its later amendments or comparable ethical standards. This article does not contain any studies with human or animal subjects performed by any of the authors.

Informed Consent Not applicable.

References

- Anttonen MJ, Hoppula KI, Nestby R, Verheul MJ, Karjalainen RO (2006) Influence of fertilization, mulch color, early forcing, fruit order, planting date, shading, growing environment, and genotype on the contents of selected phenolics in strawberry (*Fragaria × ananassa* Duch.) fruits. *J Agric Food Chem* 54:2614–2620
- Arvand M, Gholizadeh TM (2013) Gold nanorods–graphene oxide nanocomposite incorporated carbon nanotube paste modified glassy carbon electrode for voltammetric determination of indomethacin. *Sensors Actuators B Chem* 186:622–632

- Balapanuru J, Yang JX, Xiao S, Bao Q, Jahan M, Polavarapu L, Wei J, Xu QH, Loh KP (2010) A graphene oxide–organic dye ionic complex with DNA-sensing and optical-limiting properties. *Angew Chem Int Ed* 49:6549–6553
- Banks CE, Crossley A, Salter C, Wilkins SJ, Compton RG (2006) Carbon nanotubes contain metal impurities which are responsible for the “electrocatalysis” seen at some nanotube-modified electrodes. *Angew Chem Int Ed* 45:2533–2537
- Bard AJ, Faulkner LR (2004) *Electrochemical methods: fundamentals and applications*, 2nd edn. John Wiley & Sons, New Jersey
- Boyle SP, Dobson VL, Duthie SJ, Hinselwood DC, Kyle JAM, Collins AR (2000) Bioavailability and efficiency of rutin as an antioxidant: a human supplementation study. *Eur J Clin Nutr* 54:774–782
- Brolis M, Gabetta B, Fuzzati N (1998) Identification by high-performance liquid chromatography–diode array detection–mass spectrometry and quantification by high-performance liquid chromatography–UV absorbance detection of active constituents of *Hypericum perforatum*. *J Chromatogr A* 825:9–16
- Celišviūtė R, Grincienė G, Vaitekoniš Š, Venckus T, Rakickas T, Pauliukaitė R (2013) Application of carbon electrodes modified with graphene and chitosan to electrochemical sensing of ascorbate. *Chemija* 24:296–306
- Chen G, Zhang H, Ye J (2000) Determination of rutin and quercetin in plants by capillary electrophoresis with electrochemical detection. *Anal Chim Acta* 423:69–76
- Chen G, Zhang J, Ye J (2001) Determination of puerarin, daidzein and rutin in *Pueraria lobata* (Wild.) Ohwi by capillary electrophoresis with electrochemical detection. *J Chromatogr A* 923:255–262
- da Silva JG, e Silva MRL, de Oliveira AC, SouzaDe JR, Pedro Vaz CM, de Castro CSP (2012) Cathodic adsorptive stripping voltammetric determination of rutin in soybean cultivars. *J Food Comp Anal* 25:1–8
- de Oliveira IRWZ, Fernandes SC, Vieira IC (2006) Development of a biosensor based on gilo peroxidase immobilized on chitosan chemically crosslinked with epichlorohydrin for determination of rutin. *J Pharm Biomed Anal* 41:366–372
- Fatibello-Filho O, Cruz Vieira I (2000) Construction and analytical application of a biosensor based on stearic acid-graphite powder modified with sweet potato tissue in organic solvents. *Fresenius J Anal Chem* 368:338–343
- Feng X, Wang X, Xing W, Yu B, Song L, Hu Y (2013) simultaneous reduction and surface functionalization of graphene oxide by chitosan and their synergistic reinforcing effects in PVA films. *Ind Eng Chem Res* 52:12906–12914
- Ferreira Batista É, Romão Sartori E, Antigo Medeiros R, Rocha-Filho RC, Fatibello-Filho O (2010) Differential pulse voltammetric determination of sildenafil citrate (Viagra®) in pharmaceutical formulations using a boron-doped diamond electrode. *Anal Lett* 43:1046–1054
- Franzoi AC, Migowski P, Dupont J, Vieira IC (2009) Development of biosensors containing laccase and imidazolium bis (trifluoromethylsulfonyl) imide ionic liquid for the determination of rutin. *Anal Chim Acta* 639:90–95
- Franzoi AC, Spinelli A, Vieira IC (2008) Rutin determination in pharmaceutical formulations using a carbon paste electrode modified with poly (vinylpyrrolidone). *J Pharm Biomed Anal* 47:973–977
- Freitas KHG, Antigo Medeiros R, Fatibello-Filho O (2009) Voltammetric determination of rutin using a carbon composite electrode modified with copper (II)-resin. *Anal Lett* 42:881–897
- Häkkinen SH, Kärenlampi SO, Heinonen IM, Mykkänen HM, Törrönen AR (1999) Content of the flavonols quercetin, myricetin, and kaempferol in 25 edible berries. *J Agric Food Chem* 47:2274–2279
- Hendrickson HP, Kaufman AD, Lunte CE (1994a) Electrochemistry of catechol-containing flavonoids. *J Pharm Biomed Anal* 12:325–334
- Hendrickson HP, Sahafayen M, Bell MA, Kaufman AD, Hadwiger ME, Lunte CE (1994b) Relationship of flavonoid oxidation potential and effect on rat hepatic microsomal metabolism of benzene and phenol. *J Pharm Biomed Anal* 12:335–341
- Ishii K, Furuta T, Kasuya Y (2001) Determination of rutin in human plasma by high-performance liquid chromatography utilizing solid-phase extraction and ultraviolet detection. *J Chromatogr B* 759:161–168
- Jang S, Sohn H, Ko YC (2013) Synthesis and characterization of soluble alkylalcohol-derivatized graphene oxide. *Bull Korean Chem Soc* 34:1237–1239
- Jiang L, Wang R, Li X, Jiang L, Lu G (2005) Electrochemical oxidation behavior of nitrite on a chitosan-carboxylated multiwall carbon nanotube modified electrode. *Electrochem Commun* 7:597–601
- Jin M, Jeong HK, Yu WJ, Bae DJ, Kang BR, Lee YH (2009) Graphene oxide thin film field effect transistors without reduction. *J Phys D: Appl Phys* 42:135109–135113
- Kang X, Wang J, Wu H, Aksay IA, Liu J, Lin Y (2009) Glucose oxidase–graphene–chitosan modified electrode for direct electrochemistry and glucose sensing. *Biosens Bioelectron* 25:901–905
- Kim D, Jeong SW, Lee CY (2003) Antioxidant capacity of phenolic phytochemicals from various cultivars of plums. *Food Chem* 81:321–326
- Laviron E (1979) General expression of the linear potential sweep voltammogram in the case of diffusionless electrochemical systems. *J Electroanal Chem* 101:19–28
- Legnerova Z, Satinsky D, Solich P (2003) Using on-line solid phase extraction for simultaneous determination of ascorbic acid and rutin trihydrate by sequential injection analysis. *Anal Chim Acta* 497:165–174
- Leng HQ, Guo YD, Liu W, Zhang T, Deng L, Shen ZQ (2013) Determination of chlorogenic acid, rutin, scopoletin and total polyphenol in tobacco by Fourier transform near infrared spectroscopy. *Spectrosc Spect Anal* 33:1801–1804
- Liu M, Deng J, Chen Q, Huang Y, Wang L, Zhao Y, Zhang Y, Li H, Yao S (2013) Sensitive detection of rutin with novel ferrocene benzyne derivative modified electrodes. *Biosens Bioelectron* 41:275–281
- Mani V, Devadas B, Chen SM (2013) Direct electrochemistry of glucose oxidase at electrochemically reduced graphene oxide-multiwalled carbon nanotubes hybrid material modified electrode for glucose biosensor. *Biosens Bioelectron* 41:309–315
- Miao Y, Zhang Z, Gong Y, Zhang Q, Yan G (2014) Self-assembly of manganese doped zinc sulfide quantum dots/CTAB nanohybrids for detection of rutin. *Biosens Bioelectron* 52:271–276
- Nijveldt RJ, Van Nood E, Van Hoorn DE, Boelens PG, Van Norren K, Van Leeuwen PA (2001) Flavonoids: a review of probable mechanisms of action and potential applications. *Am J Clin Nutr* 74:418–425
- Notley SM, Crawford RJ, Ivanova EP (2013) Bacterial interaction with graphene particles and surfaces, advances in graphene science. M. Aliofkhaezrai (Ed.), InTech
- Pınar PT, Yardım Y, Şentürk Z (2013) Voltammetric behavior of rutin at a boron-doped diamond electrode. Its electroanalytical determination in a pharmaceutical formulation. *Cent Eur J Chem* 11:1674–1681
- Potapovich AI, Kostyuk VA (2003) Comparative study of antioxidant properties and cytoprotective activity of flavonoids. *Biochemistry* 68:514–519
- Rao M, Zheng H, Zhang L, Li Y, Duan W, Guo J, Cairns EJ, Zhang Y (2011) Graphene oxide as a sulfur immobilizer in high performance lithium/sulfur cells. *J Am Chem Soc* 133:18522–18525
- Sharma P, Tuteja SK, Bhalla V, Shekhawat G, Dravid VP, Suri CR (2013) Bio-functionalized graphene– graphene oxide nanocomposite based electrochemical immunosensing. *Biosens Bioelectron* 39:99–105
- Sheu JR, Hsiao G, Chou PH, Shen MY, Chou DS (2004) Mechanisms involved in the antiplatelet activity of rutin, a glycoside of the flavonol quercetin, in human platelets. *J Agric Food Chem* 52:4414–4418

- Song Z, Wang L (2001) Chemiluminescence investigation of detection of rutin in medicine and human urine using controlled-reagent-release technology. *J Agric Food Chem* 49:5697–5701
- Sun W, Wang X, Zhu H, Sun X, Shi F, Li G, Sun Z (2013) Graphene-MnO₂ nanocomposite modified carbon ionic liquid electrode for the sensitive electrochemical detection of rutin. *Sensors Actuators B Chem* 178:443–449
- Sun W, Yang MX, Li YZ, Jiang Q, Liu SF, Jiao K (2008) Electrochemical behavior and determination of rutin on a pyridinium-based ionic liquid modified carbon paste. *J Pharm Biomed Anal* 48:1326–1331
- Tang DQ, Wei YQ, Gao YY, Yin XX, Yang DZ, Mou J, Jiang XL (2011) Protective effects of rutin on rat glomerular mesangial cells cultured in high glucose conditions. *Phytother Res* 25:1640–1647
- Wang Y, Xiong H, Zhang X, Wang S (2010) Detection of rutin at DNA modified carbon paste electrode based on a mixture of ionic liquid and paraffin oil as a binder. *Microchim Acta* 170:27–32
- Wu SH, Sun JJ, Zhang DF, Lin ZB, Nie FH, Qiu HY, Chen GN (2008) Nanomolar detection of rutin based on adsorptive stripping analysis at single-sided heated graphite cylindrical electrodes with direct current heating. *Electrochim Acta* 53:6596–6601
- Xu C, Cai H, He P, Fang Y (2001) Electrochemical detection of sequence-specific DNA using a DNA probe labeled with aminoferrocene and chitosan modified electrode immobilized with ssDNA. *Analyst* 201: 62–65
- Yang J, Zheng J, Hu R, Chen F, Fan P, Zhong M (2014) Effect of surface modification of graphite oxide on the morphological, thermal, and mechanical properties of polyurea/graphite oxide composites. *J Appl Polym Sci* 131:39775–39783
- Yang X, Tu Y, Li L, Shang S, Tao XM (2010) Well-dispersed chitosan/graphene oxide nanocomposites. *ACS Appl Mater Interfaces* 2: 1707–1713
- Yin H, Zhou Y, Cui L, Liu T, Ju P, Zhu L, Ai S (2011) Sensitive voltammetric determination of rutin in pharmaceuticals, human serum, and traditional Chinese medicines using a glassy carbon electrode coated with graphene nanosheets, chitosan, and a poly (amido amine) dendrimer. *Microchim Acta* 173:337–345
- Zhang L, Zhang Q, Li JH (2007) Electrochemical behaviors and spectral studies of ionic liquid (1-butyl-3-methylimidazolium tetrafluoroborate) based sol-gel electrode. *J Electroanal Chem* 603:243–248
- Zhu M, Chen P, Liu M (2011) Graphene oxide wrapped Ag/AgX (X = Br, Cl) nanocomposite as a highly efficient visible-light plasmonic photocatalyst. *ACS Nano* 5:4529–4536
- Zhu Z, Sun X, Zhuang X, Zeng Y, Sun W, Huang X (2010) Single-walled carbon nanotubes modified carbon ionic liquid electrode for sensitive electrochemical detection of rutin. *Thin Solid Films* 519:928–933
- Ziaee A, Zamansoltani F, Nassiri-Asl M, Abbasi E (2009) Effects of rutin on lipid profile in hypercholesterolaemic rats. *Basic Clin Pharmacol Toxicol* 104:253–258